ELSEVIER

Polymer 42 (2001) 6271–6282

polymer

www.elsevier.nl/locate/polymer

Organo-metallic complex characterization formed when liquid epoxy-diamine mixtures are applied onto metallic substrates

S. Bentadjine[a], R. Petiaud[b], A.A. Roche[a,*], V. Massardier[a]

[a]*Inst. Nat. des Sci. Appliq. (INSA) de Lyon, Laboratoire des Matériaux Macromoléculaires, UMR CNRS No. 5627, Bât 403, 20 Avenue Albert Einstein, F-69621 Villeurbanne Cedex, France*

[b]*Service RMN/RPL, LMOPS/CNRS, BP 24, F-69390 Vernaison, France*

Received 26 July 2000; received in revised form 6 December 2000; accepted 4 January 2001

Abstract

The interfacial reactivity between metal (titanium, aluminum and gold) and epoxy-diamine prepolymer has been studied. When epoxy-diamine mixtures are applied onto gold-coated substrates, coating properties are the same as epoxy-diamine bulk ones. However when they are applied on metallic substrates (Ti and Al) and cured, an interphase, having chemical, physical and mechanical properties quite different to polymer bulk ones is formed. Nuclear magnetic resonance (NMR), FTIR, polarized optical microscopy (POM), and inductively coupled plasma spectroscopy (ICP) analyses suggest that diamine monomers chemically react and dissolve the hydrated metallic oxide layer. Metallic ions diffuse through the liquid organic layer to form a organo-metallic complex by coordination binding resulting from the electron-rich nitrogen atom of amine groups donating its lone pair to the electron-deficient metallic center.

Keywords: Epoxy-diamine prepolymer; Interphase; Organo-metallic complex

1. Introduction

The knowledge and the consideration of the 'interphase' is very important for both fundamental and practical aspects. Indeed the interphase and its properties determine the final overall properties of composite systems (practical adhesion, corrosion resistance, and durability) made of two components: the substrate and the polymeric coating.

Epoxy-diamine networks are extensively used as adhesives or paints in many industrial applications. When the precursors are applied onto metallic substrates and cured, an interphase, having chemical, physical and mechanical properties quite different to polymer bulk ones, is created between the substrate and the polymer [1].

The bibliography is not very abundant in the training area of the thick interphases. But some works show the variation of the properties of interphases created compared to the same bulk polymer. They describe the formation of new compounds responsible for the formation of this zone of different properties and behavior. Some authors have shown a catalyst effect of the substrate on the reticulation mechanisms and the prepolymer adsorption onto metallic surfaces [2,3]. Others have tempted to determine the existence of monomer/substrate specific reactions. Nigro et al. [4] have studied by using FTIR, an epoxy/BF3-monoethylamine system applied onto polished steel. The epoxy conversion rate is more important in the polymer/metal interfacial region suggesting the existence of chemical reactions with the steel surface. The epoxy prepolymer was applied onto the steel surface (without hardener), and the same phenomenon is still observed meaning that the chemical formed species at the steel surface were able to catalyze the homopolymerization of the epoxy monomer.

Kollek et al. [5] have studied, by using FTIR, the polymerization of a DGEBA/DDA system applied onto aluminum and have observed that both the DDA and the DGEBA monomers were adsorbed on the aluminum oxide surface. For the DDA monomer, the adsorption was due to the acid proton of the aluminum oxide. For the epoxy monomer, the adsorption was achieved by the oxirane (or epoxy) cycle opening. Dillingham et al. [6] have studied the polymerization of a DGEBA-TETA system applied onto aluminum by using both FTIR and XPS. Close to the polymer/metal interface, the hardener is partially protonated by aluminum

* Corresponding author. Tel.: +33-4-72-43-82-78; fax: +33-4-72-43-85-27.

E-mail address: alain-andre.roche@insa-lyon.fr (A.A. Roche).

0032-3861/01/$ - see front matter
PII: S0032-3861(01)00034-9

hydroxides. Moreover, the polymerization is catalyzed by the presence of hydroxide acid groups leading to an interphase formation.

Unfortunately, only few papers are dealing with molecular structures formed within the interphase region. As example, Kim et al. [7] have shown by studying the systems polyimide/copper at 400°C (TEM), that some copper rich particles are distributed in the polymeric matrix on a thickness from 80 to 200 μm to the polymer/metal interface. They propose that the polyamic acid reacted with copper oxide during curing by producing these particles. Kinzler et al. [8] used XPS to identify the chemical elements present at the zinc oxide/organic layer interface. They found that there is a reaction between the DICY and zinc oxide of the surface, which leads to the diffusion of the zinc molecule complexes in the polymeric matrix. The diffusion of zinc was facilitated by its complexation with the amine.

However, in such systems, chemical and physical mechanisms leading to the interphase formation are not well understood. The aim of this paper was to develop an understanding of this interphase formation and to characterize it using model epoxy-amine systems.

2. Experimental

2.1. Materials

The metallic substrates used were commercial aluminum alloy (5754) from Péchiney and titanium alloy (Ti6Al4V) from Aérospatiale. Their thicknesses were 0.516 ± 0.005 and 0.600 ± 0.005 mm, respectively. Titanium and aluminum sheets were made into rectangles of 10×50 mm^2 by die-cutting. Before any prepolymer application, the aluminum and titanium substrates were treated as shown in Table 1. A 2 nm thick amorphous Al_2O_3 oxide were formed on degreased aluminum, a 6 nm thick amorphous Al_2O_3 oxide on chemically etched aluminum, a 5 nm thick amorphous TiO_2 oxide on degreased titanium and a 15–20 nm thick amorphous TiO_2 oxide on chemically etched titanium [9–13]. Immediately after surface treatments, specimens were stored in an air-conditioned room at 22 ± 2°C and 55 ± 5% R.H. for 1 h. Some aluminum sheets were coated with gold (≈100 nm) using a SCD005 Sputter Coater from Bal-Tec.

Table 1
Surface treatment of aluminum and titanium alloys

Alloy	Treatment	Description
Aluminum	Degreasing	Ultrasonically degreased in acetone for 10 min and in ethyl acetate for 10 min, wiped dry
	Chemical etching	Degreased and submerged in a solution of 250 g l^{-1} sulfuric acid, 50 g l^{-1} chromium acid, 44 g l^{-1} aluminum sulfate, at 60°C for 20 min; rinsed in running tap water for 1 min, standed in deionized water for 5 min and wiped dry
Titanium	Degreasing	Ultrasonically degreased in acetone for 10 min and in ethyl acetate for 10 min, wiped dry
	Chemical etching	Degreased and submerged in a solution of 10 g l^{-1} ammonium bifluoride, room temperature for 2 min; rinsed in running tap water for 1 min, standed in deionized water for 5 min and wiped dry

Table 2
Cure cycles for different epoxy/diamine systems

System	Cure cycle
DGEBA + IPDA	3 h at 20°C; 20 → 60°C (2°C min^{-1}); 2 h at 60°C; 60 → 140°C (2°C min^{-1}); 1 h at 140°C; 140 → 190°C (2°C min^{-1}); 6 h at 190°C; cooling in the oven to 20°C (1°C min^{-1})
DGEBA + MCDEA	3 h at 20°C; 20 → 60°C (2°C min^{-1}); 2 h at 60°C; 60 → 160°C (2°C min^{-1}); 4 h at 160°C; 160 → 190°C (2°C min^{-1}); 9 h at 190°C; cooling in the oven to 20°C(1°C min^{-1})

The epoxy prepolymer used was a diglicidyl ether of bisphenol A (DGEBA, $\overline{n} = 0.03$, $M = 348.52$ g mol^{-1} DER 332 from Dow Chemical). Diamine hardeners used were the isophorone-diamine (IPDA or 3-aminomethyl-3,5,5-trimethylcyclohexylamine) from Fluka and the 4,4′-methylenebis[3-chloro 2,6-diethylaniline] (MCDEA) from Lonza. The epoxy prepolymer and curing agents were used without further purification. The stoichiometric ratio (a/e) (amino hydrogen/epoxy) used was equal to 1. This ratio was calculated using a functionality of four for the diamine and two for the epoxy monomers. The epoxy-amine bulk or coating cure cycle [14,15] was adapted to obtain both the maximum cure conversion (i.e. the highest glass transition temperature denoted T_g^∞) and the thickest interphase (Table 2).

Bulk polymers were prepared by pouring the corresponding mixture in a $10 \times 10 \times 100$ mm^3 PTFE mould cavity. After curing and cooling down, specimens were sliced to the desired thickness with a mechanical diamond saw. The same mixture was also applied on treated metallic sheets to obtain the desired coating thickness (Fig. 1) by using sacrificial substrate of desired thickness. After curing and cooling down, coating thicknesses (from 40 to 1500 μm) were determined using a EG-100 Digital Linear Gauge (from Ono Sokki, Japan) having a ±2 μm sensitivity.

To characterize changes in monomers, (leading to the interphase formation), either liquid DGEBA or liquid IPDA monomer were each applied between two chemically treated metallic substrates (50×50 mm^2) to form a 100–150 μm thick liquid film and kept at room temperature during 3 h in a desiccator under continuous nitrogen flow to prevent any monomer carbonation or oxidation [16]. Then 'modified' monomers were scraped from the metallic substrates with a PTFE spatula and stored in polyethylene vials under a nitrogen atmosphere until using.

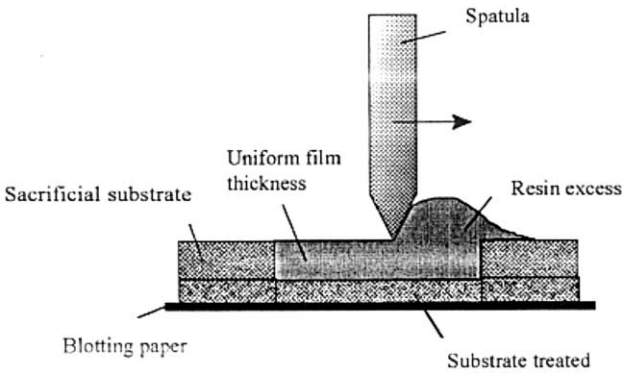

Fig. 1. Preparation of coated substrates.

2.2. Characterization

2.2.1. Nuclear magnetic resonance spectroscopy (NMR)

Nuclear magnetic resonance (NMR) was carried out with a BRUKER DRX 400 spectrometer operating at 400.13 MHz for ^{1}H and 100.62 MHz for ^{13}C. Analyses were carried out either at room temperature for 1D spectra and at 298 K for 2D spectra, using deuterated water in which pure or modified IPDA monomers were perfectly soluble. Usually, 200 mg of pure or modified monomers were added to 0.75 ml of deuterated water. Due to an excess of IPDA in modified IPDA monomers, it was not possible to know the exact concentration of complexes in NMR solutions. As intermolecular H bonds are present in aqueous solutions of substances containing IPDA, chemical shifts can evolve with dilution and only give semi-quantitative results. 1D spectra were obtained with a QNP probe. For 2D spectra, a broad-band probe with field gradient on z-axis was used, with a COSY-GS sequence for ^{1}H–^{1}H correlation and HMQC-GS and HMBC-GS for ^{1}H–^{13}C correlation with 28 and 64 scans, respectively.

2.2.2. Thermal analysis (DSC)

The glass transition temperature of the DGEBA/diamine bulk (T_g^{∞}) and coatings (T_g) were determined by using a differential scanning calorimeter (Mettler Toledo DSC 30). Sealed aluminum pans containing 15–20 mg epoxy materials were heated from −50 to 250°C at a rate of 10°C min^{-1} under a continuous flow of U grade argon. The calorimeter was calibrated with both indium and zinc standards. The glass transition temperature was determined by the onset point with a ±0.5°C sensitivity. To evaluate the variation in T_g versus the coating thickness, the $(T_g)_{eq}$ value at the thickness (i) was calculated using

$$(T_g)_{eq} = \frac{h_i T_{g_i} - h_{i-1} T_{g_{i-1}}}{h_i - h_{i-1}}, \tag{1}$$

where T_{g_i} corresponds to the T_g of a h_i thick coating and $T_{g_{i-1}}$ value corresponds to the glass transition temperature of a h_{i-1} thick coating.

2.2.3. Infrared and near-infrared spectroscopy (FTNIR)

An infrared spectrometer (FTIR Magna-IR 550 from Nicolet) was used with Omnic FTIR software. An Ever-Glo™ source was used along with a KBr beam-splitter and DTGS-KBr or MCT/A detectors. The mid-infrared spectra were recorded in the 400–4000 cm^{-1} range and in the 4000–7000 cm^{-1} range for the near-infrared. A transmission accessory was used for bulk or free-standing film characterization. For the bulk material, KBr (Spectronorm for spectroscopy IR from Prolabo) was mixed in a 1:100 ratio with the various epoxy resins, which have been ground cryogenically. This mixture was then pressed under vacuum to obtain disks. Pure KBr disks were used as background. For each analysis, 64 or 96 scans were collected at 4 cm^{-1} resolution.

Cure conversions for epoxy (X_e) and amine (X_a) groups were calculated, respectively, by using the 4530 cm^{-1} epoxy combination band [17] and the 6500 cm^{-1} amine band [18]. The 4623 cm^{-1} aromatic C–H ring stretch combination band was considered as reference. Thus, the amine and the epoxy conversions were determined using the ratio of their respective band area (A) by

$$X_a = 1 - \frac{(A_{6500}/A_{4623})_t}{(A_{6500}/A_{4623})_{t=0}} \quad \text{and} \qquad X_e = 1 - \frac{(A_{4530}/A_{4623})_t}{(A_{4530}/A_{4623})_{t=0}}. \tag{2}$$

Once again, to evaluate the X_a and X_e variation versus the coating thickness we calculate the $(X_a)_{eq}$ and $(X_e)_{eq}$ values at the thickness (i) using

$$(X_{a,e})_{eq} = \frac{h_i (X_{a,e})_i - h_{i-1} (X_{a,e})_{i-1}}{h_i - h_{i-1}}, \tag{3}$$

where $(X_{a,e})_i$ corresponds to the $(X_{a,e})$ of a h_i thick coating and $(X_{a,e})_{i-1}$ value corresponds to the conversion of a h_{i-1} thick coating.

According to Lin et al. [14], homopolymerization phenomena were studied, for some systems, by using the ratio of the ether/phenyl band area (A_{1120}/A_{830}).

2.2.4. Inductively coupled plasma spectroscopy (ICP)

An ICP spectrometer (Modula by Spectro Analytical Instruments) was used with a 2.5 kW plasma generator at 27 MHz and with UV (0.75 m, 2400 grooves mm^{-1}; 160–480 nm) monochromator, UV (0.75 m, 3600 grooves mm^{-1}) polychromator and visible (0.75 m, 1200 grooves mm^{-1}) polychromator. A cross-flow nebulizer was used to introduce the liquid sample. Dionized water was used as solvent in 1:100 ratio.

2.2.5. Polarized optical microscopy (POM)

Drops of modified IPDA diamine were confined between two glass plates and mounted on a hot plate accessory under a POM apparatus (Laborlux 12POLS from Leica equipped with a hot plate FP82 from Mettler and a CCD-IRIS color

video camera from Sony). Samples were heat from 30 to 190°C at 10°C min^{-1}.

2.2.6. Size exclusion chromatography (SEC)

A Waters apparatus was used with a double detection (UV Waters 484 Tunable Absorbance Detector at $\lambda = 254$ nm and Waters 410 differential Refractometer) and a Waters 510 HPLC pump. The elution solvent used was tetrahydrofuran (THF) and the separation was carried out on two styrene-divinyl benzene columns (Nucleogel 100-5 and 500-5 from Macherey–Nagel) with a 1 ml min^{-1} flow rate. The mass average molar mass calibration curve was constructed from monodispersed polystyrene standards.

3. Results and discussion

3.1. Physical and chemical properties of coatings

Properties of DGEBA/IPDA and DGEBA/MCDEA bulks are listed in Table 3. Equivalent glass transition temperatures versus the coating thickness are plotted in Fig. 2 for the system DGEBA + IPDA cured on three different substrates (chemically etched aluminum or titanium and gold). For coatings applied onto gold-coated substrates, the $T_{g_{eq}}$ were equal to the T_g^{∞} of the cured bulk material whatever the coating thickness was. On the contrary, for coatings applied either on titanium or aluminum, only thick coatings ($h_c \geq 0.7$ mm for titanium and $h_c \geq 0.285$ mm for aluminum) have T_g values close to the bulk one (T_g^{∞}). For thinnest coatings ($\leq$0.4 mm for titanium and $\leq$0.2 mm for aluminum) $T_{g_{eq}}$ values are quite constant ($\approx$ 129°C for titanium and $\approx$ 110°C for aluminum) but values were very different to the bulk ones. For coating thicknesses between $0.4 < h_c < 0.7$ mm for titanium and $0.2 < h_c < 0.3$ mm for aluminum, a gradient region was observed. The interphase being defined as the region where the properties are different to the bulk ones, an interphase thickness of 0.7 and 0.4 mm are observed for titanium and aluminum, respectively. A similar behavior was also observed with the MCDEA amine (Fig. 3), i.e. the formation of a thick interphase at the metallic surface vicinity. Thermal analyses show that physical properties of these films are very different from the bulk ones unless for the outer part of very thick coatings.

The equivalent amine $(X_a)_{eq}$ and epoxy $(X_e)_{eq}$ extent rates are plotted versus the coating thickness in Fig. 4 for DGEBA + IPDA cured on chemically etched titanium and gold. For both cases (titanium and gold-coated substrates) X_e is independent of coating thickness and is close to 100%. That means that all epoxy groups have completely reacted. When coatings were applied onto gold-coated substrates, the amine (X_a) conversions were always equal to 100%. For such coatings applied onto gold, X_a and X_e were equal to 1. Then we can deduce that, whatever the coating thickness may be, coating properties were the same as the bulk ones, i.e. there is no chemical reaction between gold and either the DGEBA epoxy or the IPDA diamine monomers. In the case of titanium substrate, only for coatings thicker than 0.7 mm, X_a reaches the value of the bulk material (100%). For coatings thinner than 0.4 mm X_a was 84%. In other words some of amine groups have not been consumed during the amine-epoxy reaction. Since for these thin coatings X_e was equal to 1, we have studied the homopolymerization phenomena according to Lin [19]. DGEBA/IPDA bulk materials and 100 μm thick coatings on titanium of

Table 3
Physical and chemical properties of bulk materials

	DGEBA/IPDA	DGEBA/MCDEA
Glass transition temperature T_g^{∞} (°C)	163 ± 1	187 ± 1
Epoxy extent rate X_e (%)	99 ± 1	99 ± 1
Amine extent rate X_a (%)	99 ± 1	99 ± 1

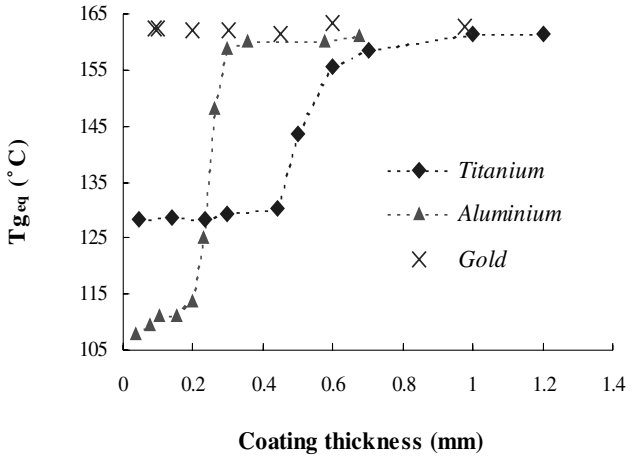

Fig. 2. Equivalent glass transition temperature $(T_g)_{eq}$ as a function of the DGEBA/IPDA (a/e = 1) coating thickness for chemically etched aluminum, chemically etched titanium and gold-coated substrates.

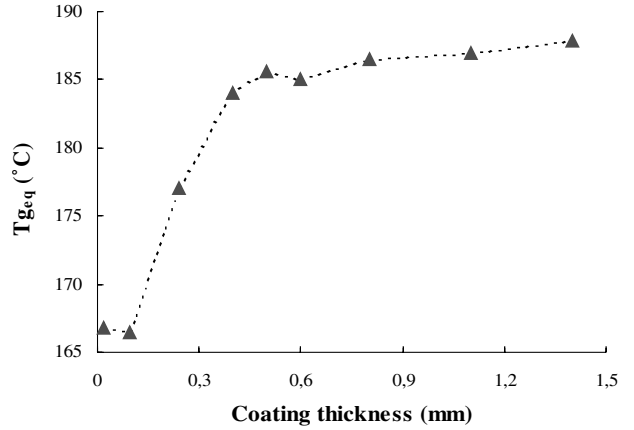

Fig. 3. Equivalent glass transition temperature $(T_g)_{eq}$ as a function of the DGEBA + MCDEA (a/e = 1) coating thickness for chemically etched titanium substrates.

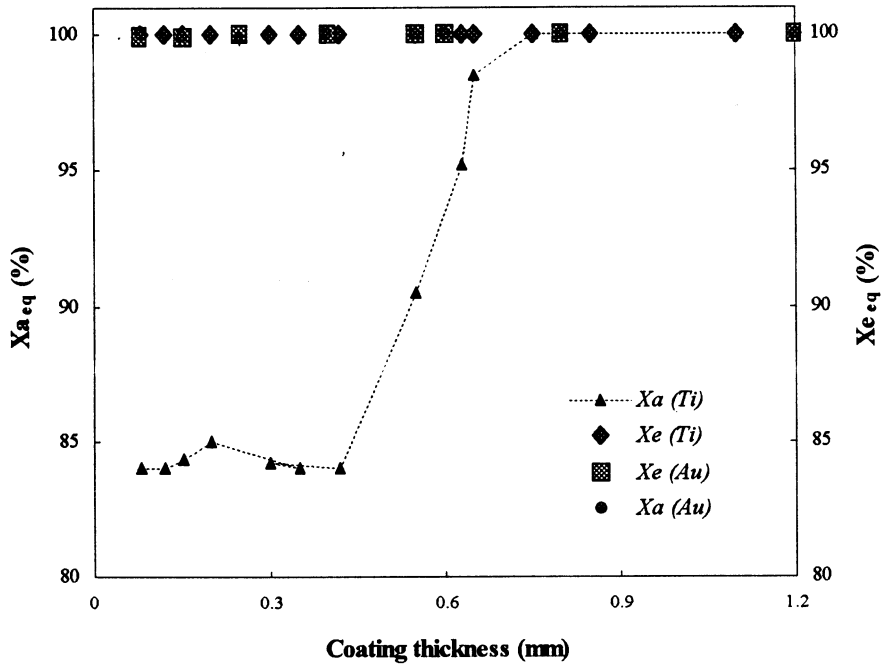

Fig. 4. Variation of the epoxy conversion (X_e) and amine conversion (X_a) versus the thickness of DGEBA/IPDA coatings applied onto chemically etched titanium and gold-coated substrates.

various stoichiometric ratio (a/e = 0.7, 1 and 1.3) were prepared and analyses using FTIR. Variations of the ether/phenyl band area (A_{1120}/A_{830}) ratio were plotted versus the stoichiometric ratio (a/e) as represented in Fig. 5. Undoubtedly, the homopolymerization phenomena increases when DGEBA/IPDA were applied onto titanium substrate. These homopolymerization increase may be responsible to the observed $X_e = 1$ while $X_a = 0.84$ for the thinnest coatings on titanium.

FTIR analyses show that chemical properties of thin films are very different from the bulk ones. The significant differences observed for both chemical and physical properties of these coatings, compared to the bulk ones, means that a polymer/substrate interphase is created. To characterize chemical changes occurring, liquid DGEBA or IPDA monomers were placed between two chemically treated metallic substrates and kept at room temperature for 3 h. Then, the modified monomers were scraped from their metallic

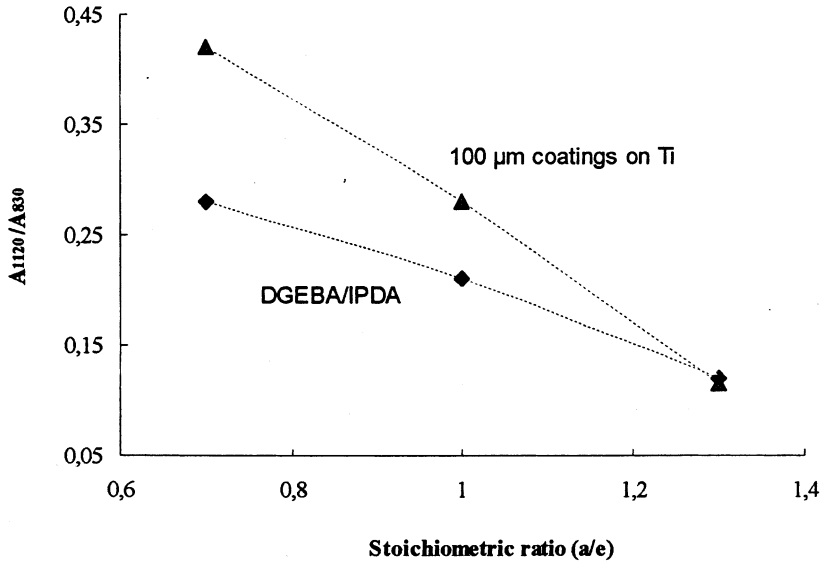

Fig. 5. Variation of the ether/phenyl band area (A_{1120}/A_{830}) ratio versus the stoichiometric ratio for DGEBA/IPDA bulk materials and 100 μm thick coatings on titanium of various stoichiometric ratio (a/e = 0.7, 1 and 1.3).

substrates with a PTFE spatula and compared to the pure monomers.

3.2. Modified monomers characterization.

All pure monomers (DGEBA and IPDA) are transparent. No color change of the DGEBA monomer after application either on titanium or aluminum. No color change was also observed when IPDA monomer has been applied onto a gold-coated substrate. However IPDA modified monomers from both aluminum and titanium became milky white. After two hours in test tubes, separation was observed (Fig. 6). The floating part remained transparent while the precipitate was milky white. One drop of the precipitate from either aluminum or titanium modified IPDA was placed between two glass plates and observed using a polarized optical microscope (POM) (Fig. 7). Crystals in the modified IPDA liquid drop were observed corresponding to the precipitation of a new chemical product when its concentration is higher than the solubility parameter. Obviously, a new chemical specie has been created when the diamine monomer stay in contact with metallic surfaces. Fig. 8 represents ICP spectra of pure IPDA and the precipitate part of the aluminum/titanium modified IPDA. The presence of either aluminum or titanium stands clearly in modified IPDA monomer spectra translating a partial dissolution of the oxide and/or hydroxide metallic surface by the diamine monomer, followed by a metallic ion diffusion within the liquid diamine monomer. Fig. 9 contains the UV and RI SEC spectra obtained from pure 'MCDEA' monomer and modified MCDEA with titanium and aluminum substrates. New RI small peaks were observed which correspond to $\overline{M}_w = 1014$ g mol^{-1} for titanium and $\overline{M}_w = 1011$ g mol^{-1} for aluminum. These values are twice higher than the pure MCDEA monomer mass average molar mass ($\overline{M}_w = 489$ g mol^{-1}).

At this point, it was interesting to summarize the former work. When DGEBA epoxy monomer was applied on titanium, aluminum or gold, no chemical reaction was observed. When IPDA monomer was applied onto gold-coated substrate, no chemical reaction was observed too. On the contrary, when liquid IPDA monomer was applied onto either titanium or aluminum substrates, chemical reaction was observed leading to a partial basic dissolution of the metallic surface followed by the metallic ion diffusion. Metallic ions react with the amine monomer to form a new species, which crystallizes when the solubility parameter value is reached. The mass average molar mass of this new specie is twice the pure monomer one. However, the chemical bond nature leading to this new specie is unknown. According to several authors [20–23], a complex formation between amine groups and metallic ions is highly suspected. To fully identify chemical bonds that may appear between the IPDA monomer and metallic ions, NMR was used.

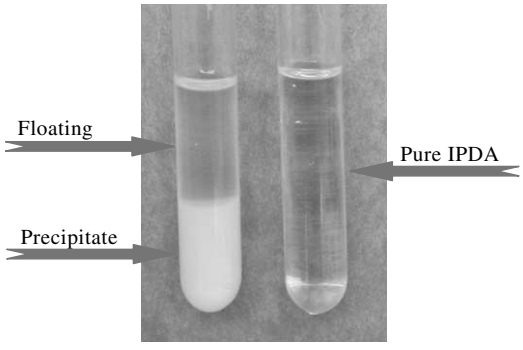

Fig. 6. Visual aspect of pure IPDA monomer and modified IPDA monomer after application on aluminum or titanium substrate.

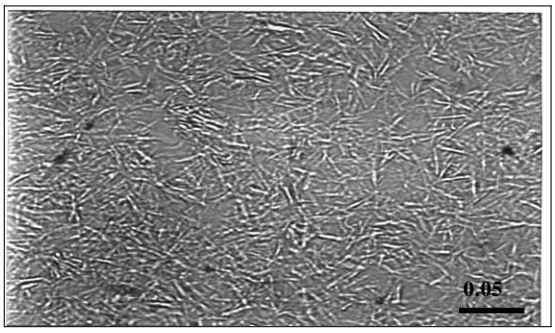

Fig. 7. POM photograph of modified IPDA monomer after application on aluminum substrate.

3.3. NMR study.

3.3.1. Molecular modeling for IPDA

Pure IPDA monomer supplied by 'Fluka' was a mixture

Table 4
Assignment of the different peaks of the ^{1}H spectrum obtained for the pure IPDA/D_2O

Isomer *cis* ($C9_{eq}$)	Isomer *trans* ($C9_{ax}$)	δ (ppm)	J (Hz)
H1 (ax)		2.926	11.7 and 3.5
	H1′ (ax)	2.856	11.8 and 3.5
	H9′a	2.604	13.4[a]
	H9′b	2.533	13.4[a]
H9a		2.286	13.2
H9b		2.271	13.2
	H2′ (eq)	1.754	12.9
	H6′ (eq)	1.58	Complex peak
H6 (eq)		1.56	Complex peak
H2 (eq)		1.54	Complex peak
	H4′ (eq)	1.349	14.2
H4 (eq)		1.094	13.5
3H7		1.024	
H4 (ax)		0.995	
3H10	3H7′	0.981	
3H8		0.923	
	3H8′	0.92	
	H4′ (ax)	0.92	
H6 (ax)		0.867	12.5
	3H10′	0.855	
	H6′ (ax)	0.836	
H2 (ax)		0.774	12.5
	H2′ (ax)	0.74	

[a] = W with H_2'.

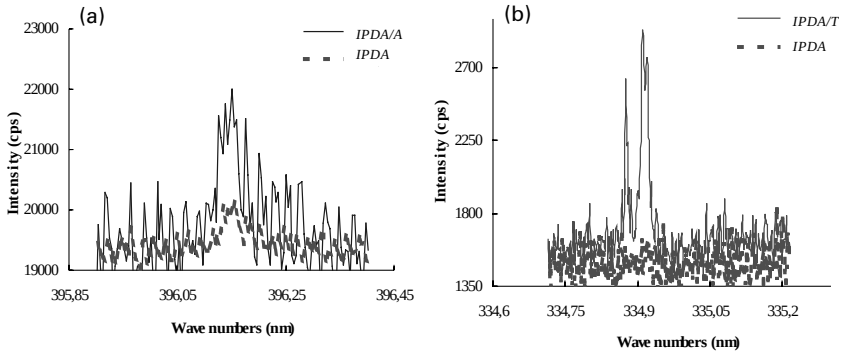

Fig. 8. ICP spectra of pure IPDA and modified IPDA monomers after application on (a) aluminum and (b) titanium substrates.

of 25% *trans* (–CH_2–NH_2 → axial 'C9′ ax') and 75% *cis* (–CH_2–NH_2 → equatorial 'C9eq') isomers. We have calculated, with energy minimization, using Céruis2 software, the different configurations for every IPDA isomers. The corresponding conformations of these two isomers are shown in Fig. 10 with the carbon atom numbering used in the following work. The same numbering is used for the *cis* and *trans* isomers but the subscript '′' was used for the *trans* one. The distance between the two nitrogen atoms of the amine groups has been calculated to be 5.3 and 5.8 Å for the *cis* and *trans* isomer, respectively.

3.3.1.1. NMR study of pure IPDA. IPDA has a structure very similar to IPDI (3-aminomethyl-3,5,5-trimethylcyclohexylisocyanate or isophorone diisocyanate) which was studied by Gerard [24,25]. So, some conclusions can be deduced from previous work carried out on IPDI.

The 1D ^1H and ^{13}C spectra show that both isomers are existing (Fig. 11). Indeed, on the ^{13}C spectrum, there are 19 peaks for 10 carbons. For the ^1H spectrum, there is a complex signal between 2.900 and 2.800 ppm for H1 and H1′ protons and two groups of peaks (AB patter) between 2.650 and 2.500 ppm and between 2.325 and 2.225 ppm for H9 and H9′. The integration of these two peaks leads to a composition of 73.4% for the isomer *cis* and 26.6% for the *trans* one. These ratios are in good agreement with data from Fluka who supplied the product. They are also very close to the one found by Gerard [15,16] for the IPDI and are in agreement with steric effects. Indeed, the CH_2–NH_2 or CH_2–N═C═O groups corresponding to C9 being rather big, an equatorial position (*cis*) is more probable. This position is rather stable, as when complexed by the Al or Ti metals, the *cis*/*trans* ratio of the IPDA structure does not evolve at least in water.

3.3.1.1.1. ^1H–^1H proton correlation. The 2D spectra used for making the correlation are shown in Fig. 12. Thanks to the H1 proton of the *cis* complex that appears as a triplet of triplets centered at 2.926 ppm. It is possible to assign $H2_{eq}$ and $H6_{eq}$ to the peaks between 1.500 and 1.600 ppm, and also $H2_{ax}$ and $H6_{ax}$ to peaks between 0.700 and 0.970 ppm. A coupling is also present between $H2_{eq}$ + $H6_{eq}$ and $H4_{eq}$ at 1.094 ppm. It corresponds to a part of an AB system with $H4_{ax}$ at 0.995 hidden covered by the H7 and H10 methyl protons, which are, respectively, coupled with $H6_{ax}$ and $H2_{ax}$. A coupling between the two H9 and the three H10 protons is also present. The spectra corresponding to isomer *trans* can be interpreted in the same way.

The assignment of the different peaks are summarized in Table 4. Moreover, one part of the study was focused on protons H9 and H9′. For both *cis* and *trans* compounds, protons H9 and H9′ lead to an AB spectrum showing non-equivalent –CH2– protons. A zoom of the region 2.700–2.450 ppm (F1) and 0.890–0.660 ppm (F2). Fig. 13 shows a coupling between the proton H9′ (called H9′b) and the proton $H2'_{ax}$. Most probably, it is a W coupling that implies the conformation drawn in Fig. 13(a). Moreover,

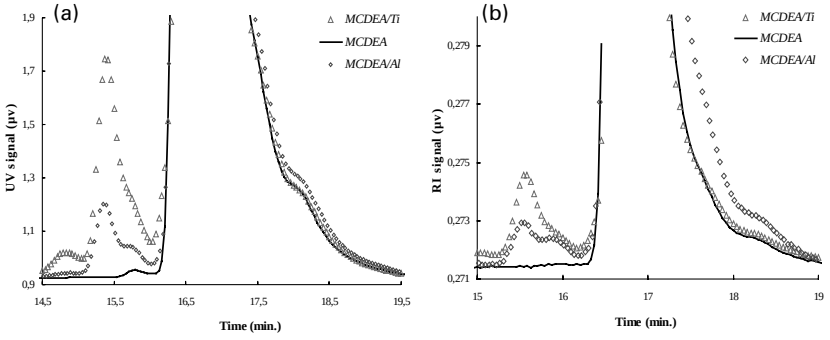

Fig. 9. (a) UV and (b) RI SEC spectra of pure MCDEA and the modified MCDEA with titanium and aluminum.

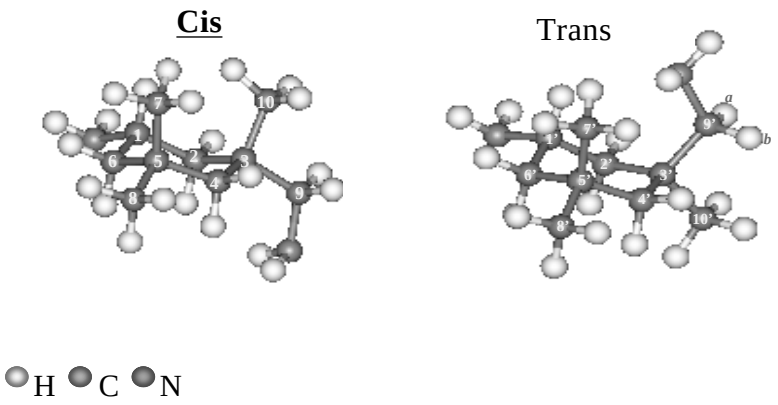

Fig. 10. *cis* and *trans* IPDA isomer conformations and carbon atom labeling.

the non-equivalence, of the H9 proton shows that compound *cis* is in a blocked conformation (probably the one drawn in Fig. 13(b) with two protons having a very similar neighboring (Table 5).

3.3.1.1.2. $^{1}H-^{13}C$ correlation. First, by the ^{1}J correlation between protons and carbons were determined with an HMQC experiment. It was followed by an HMBC experiment for finding the long-range correlation. Fig. 14 shows the 2D spectrum obtained with the HMQC experiment. It enables to assign most of the carbons in

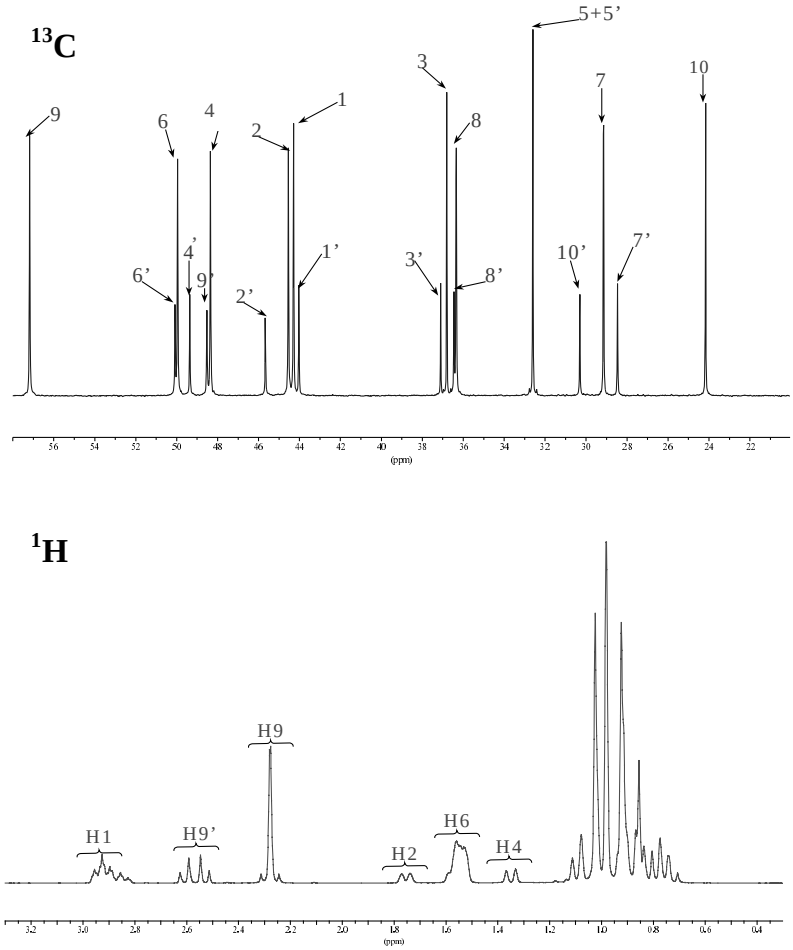

Fig. 11. ^{1}H and ^{13}C NMR spectra of pure IPDA

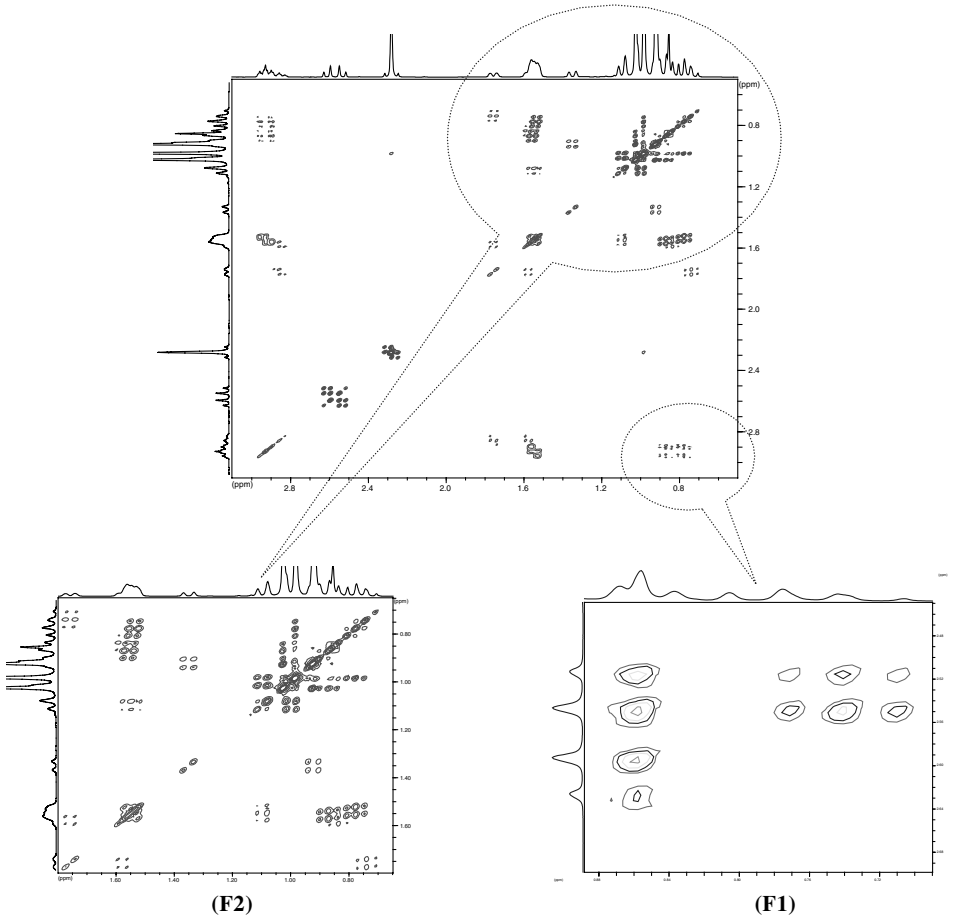

Fig. 12. ^{1}H 2D NMR spectrum for the pure IPDA/D_2O and different close up.

Table 5
Assignment of the different peaks of the ^{13}C spectrum obtained for the pure IPDA/D_2O

No. of peak	δ (ppm)	Majority (C9 eq)	Minority (C9′ ax)
1	55.59	C9	
2	48.49		C6′
3	48.37	C6	
4	47.77		C9′
5	46.93		C4′
6	46.77	C4	
7	44.07		C2′
8	42.95	C2	
9	42.70	C1	
10	42.44		C1′
11	35.52		C3′
12	35.21	C3	
13	34.87		C8′
14	34.75	C8	
15	31.01	C5	C5′
16	28.72		C10′
17	27.56	C7	
18	26.88		C7′
19	22.58	C10	

agreement with the previous assignments carried out with the $^{1}H-^{1}H$ NMR. Fig. 15 displays the results of the HMBC experiment. The C3 and C3′ quaternary carbons can be assigned thanks to their respective coupling with H9 and H9′ protons. Also C5 and C5′ can be assigned thanks to their respective correlations with H7 and H8 and with

Table 6
Chemical shifts as observed by ^{13}C NMR analysis for Al and Ti modified IPDA monomers

cis isomer (C9eq)	*trans* isomer (C9′ ax)	$\Delta\delta$ (ppm)[a]	
		Al	Ti
C1		0.44	0.22
	C1′	0.47	0.23
C2		0.6	0.18
	C2′	0.68	0.22
C3		0.3	0.12
	C3′	0.24	0.1
C9		0.44	0.16
	C9′	0.39	0.15
C10		0.23	0.1
	C10′	0.29	0.1
	C4′	−0.5	−0.29

[a] $\Delta\delta = \delta$ (IPDA/Metal) − δ (IPDA).

Fig. 13. Conformation (a) of the isomer *trans* around carbons C9′ and C3′ and (b) of the isomer *cis* around carbons C9 and C3 (in both cases the denominations (a) and (b) for protons 9 and 9′ are arbitrary).

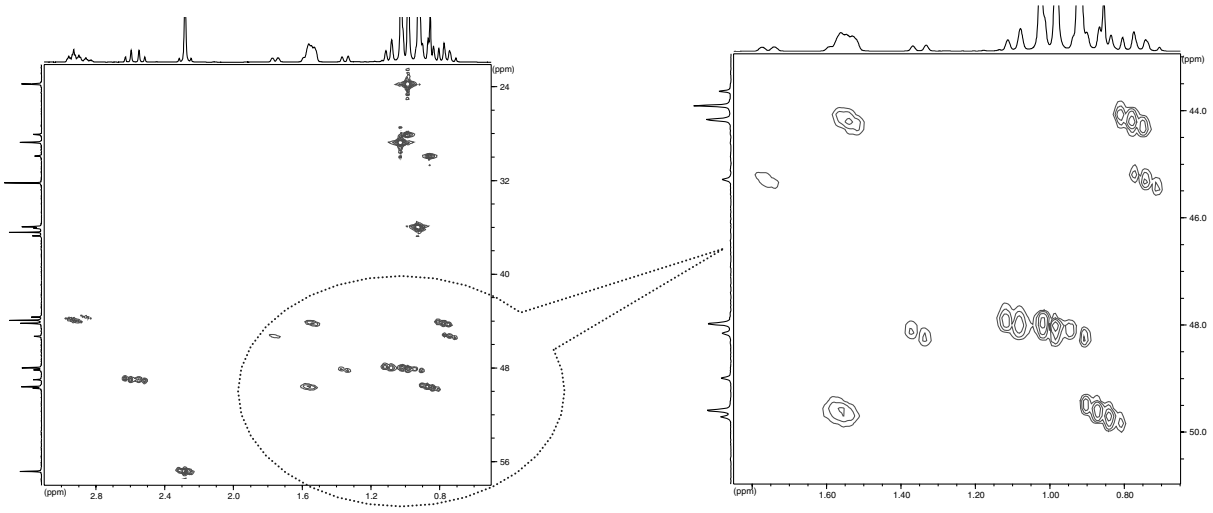

Fig. 14. HMQC D2 spectra of correlated protons and carbons of the pure IPDA/D_2O.

protons H7′ and H8′. Moreover, couplings of C6 with H7 and H8, of C6′ with H7′ and H8′, of C2 with H10 and of C2′ with H10′ with previous assignments including those of H6, H6′, H2 and H2′ are evidenced. The multiplicities of ^{13}C signals were determined with the DEPT technique.

3.3.1.2. Study of the 'IPDA + Al' and 'IPDA + Ti' complexes. Although their ^{1}H and ^{13}C NMR spectra are rather close, some significant differences can be noticed (Figs. 16 and 17). For the ^{1}H spectrum, the main difference is observed on the IPDA + Ti spectrum where both H9′ are equivalent (Fig. 16). The ^{13}C NMR spectra displayed in Fig. 17 show that the metal influences chemical shifts of both complexes and their variations are reported in Table 6. For the used concentrations (about 1:4), the shifts are higher with Al ($\Delta\delta Al/\Delta\delta Ti = 3$). As intermolecular H bonds are present in various IPDA aqueous solutions, chemical shifts can evolve with

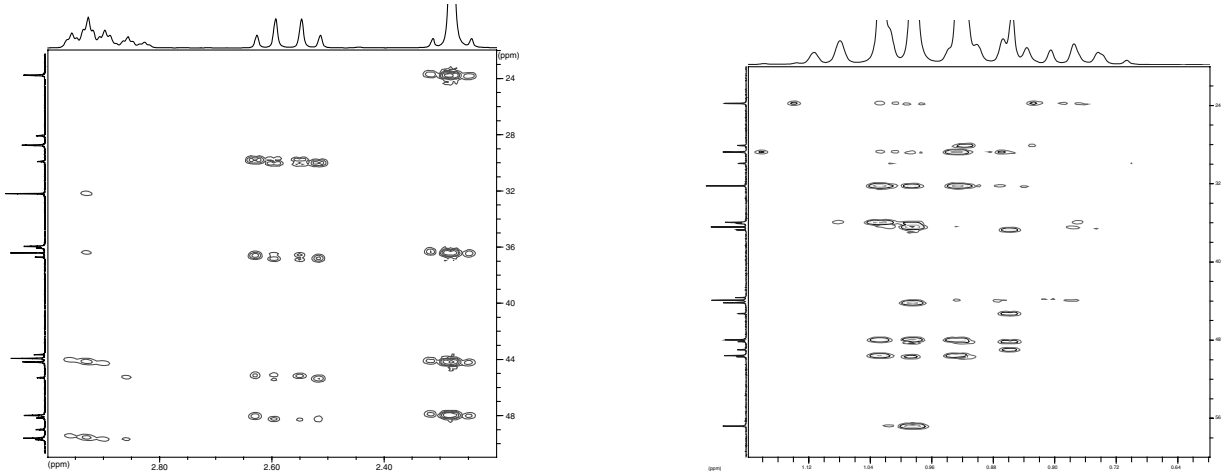

Fig. 15. HMBC D2 spectra of correlated carbons and protons located at two or three connections of the IPDA/D_2O.

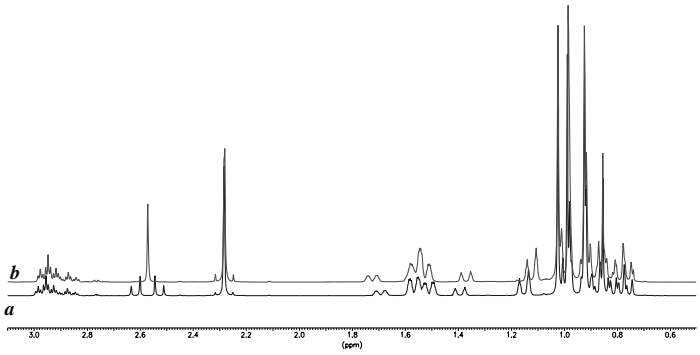

Fig. 16. ^{1}H NMR spectra for (a) modified aluminum IPDA 'IPDA/Al' and (b) modified titanium IPDA 'IPDA/Ti'.

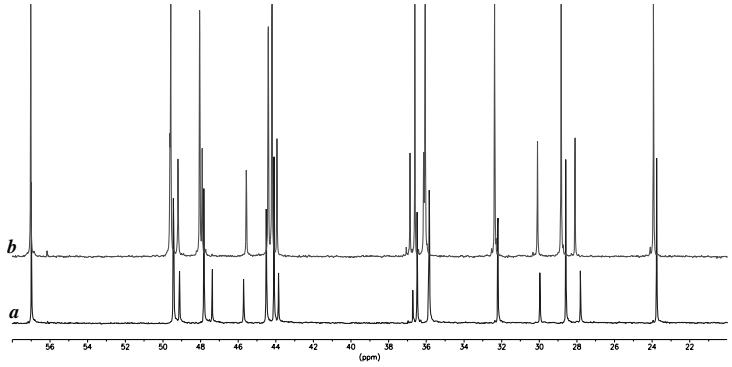

Fig. 17. ^{13}C NMR spectra for (a) modified aluminum IPDA IPDA/Al and (b) modified titanium IPDA IPDA/Ti.

dilution. This point will be discussed in a future paper. Nevertheless, the chemical shift may be characteristic of the metal electro negativity (Al is more electropositive than Ti). The acidity of Lewis of these two metals (aluminum and titanium) can also play a significant role.

The effect of both metal corresponds to a deshielding effect of carbons C1, C1′, C2, C2′, C3, C3′, C9, C9′, C10 and C10′ for both *trans* and *cis* isomers. For the *trans* isomer, a shielding of C4′ is also observed. It is noted that the effect of metal in both cases (Al and Ti) is a sum effect since we certainly have a balance effect between the complex and the remaining unmodified IPDA diamine monomer.

As could be expected, it is mainly the carbons between the two nitrogenous and also the C10 and C10′ close to nitrogen that are the most affected and undergo a decrease of their electronic density during the complexation. When comparing the spectra of IPDA with its Ti and Al complexes, it appears that the rotating movement of the $C_{(9)}H_{(9)2}-NH_2$ is not possible because the 2H are not equivalent. Moreover, the AB pattern of the $H_{(9)a}$ becomes a singlet in the Ti complex. It means that in this last complex the $2H_{(9)a}$ are about equivalent with the same electronic density. So, the effect of the complexation on the chemical shifts is two to three times more important with Al than with Ti and both nitrogen atoms are equally affected by the complexation as depicted in Fig. 18.

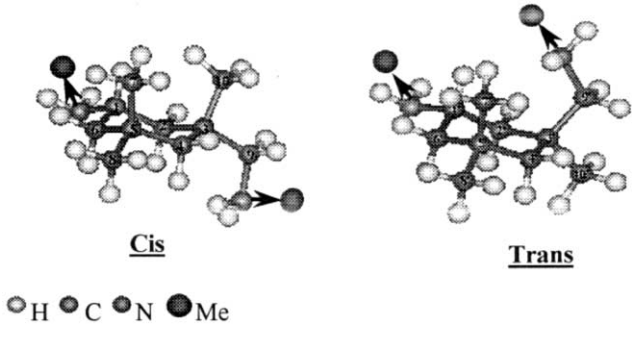

Fig. 18. Reaction pathway of the nitrogen/metal reaction.

4. Conclusion

When epoxy-diamine are applied onto metallic substrates, an interphase of important thickness between the coating and the metallic surface is created. Formation mechanisms of this interphase region have been unknown until now. Using different techniques, we have been able to propose these mechanisms. Partial dissolution of the oxide/hydroxide metallic substrate surface is observed either for aluminum or titanium substrates, whatever may be the surface treatment. This point has been described elsewhere [26–29]. Then metallic ions diffuse within the liquid mixture and react with the amine groups of the curing

agent to form organo-metallic complexes by coordination. With the help of NMR, we have found that the two nitrogenous groups of the diamine monomer are affected by this reaction with metallic ions. These organo-metallic complexes react with the DGEBA epoxy monomer to form a new epoxy network inducing chemical, physical and mechanical properties quite different to polymer bulk ones.

References

[1] Sharp LH. J Adhes 1972;4:51.
[2] De'neve B. Ph.D. thesis, Ecole Nationale Supérieure des Mines de Paris, 1993.
[3] Péchereaux. Ph.D. thesis, Université de Haute Alsace, 1990.
[4] Nigro J, Ishida H. J Appl Polym Sci 1989;38:2191.
[5] Kollek H. Int J Adhes Adhesives 1985;5:75.
[6] Dillingham RG, Boëro FG. J Adhes 1987;24:315.
[7] Kim YH, Walker GF, Kim J, Park J. J Adhes Sci Technol 1987;1:331.
[8] Kinzler M, Grunge DM, Blank N. J Vac Sci Technol 1992;A10:2691.
[9] Cuntz JM. Ph.D. thesis, CNAM de Paris, 1986.
[10] Roche AA. Technical report, AFWAL-TR-80-4004, Wright Patterson Air Force Base, Ohio, 1980.
[11] Roche AA, Solomon JS, Baun WL. Appl Surf Sci 1981;7:83.
[12] Roche AA, Solomon JS. Proceedings of the Eighth International Vacuum Congress, Le Vide, les couches minces, Supplément, Volume II, vol. 201, 1980;445
[13] Roche AA. Ph.D. thesis, Université de Lyon, 1983.
[14] Sindt O, Perez J, Gerard JF. Polymer 1995;37:2989.
[15] Gérard-reydet E. Ph.D. thesis, INSA de Lyon, 1996.
[16] Burton BL. J Appl Polym Sci 1993;47:1821.
[17] Miller CE. 1991;26:277.
[18] Mijovic J, Andjelic S. Polymer 1995;36:3783.
[19] Lin YG, Sautereau H, Pascault JP. J Polym Sci 1986;24:2171.
[20] Wernick S, Pinner R editors. Les traitements de surface et la finition de l'aluminium et de ses alliages. Paris: Eyrolles, 1962.
[21] Kim YH, Walker GF, Kim J, Park J. J Adhes Sci Technol 1987;1:331.
[22] Kinzler M, Grunge M, Blank N, Shenkel H, Scheffler I. J Vac Sci Technol 1992;10(4):2691.
[23] Kuo JS, Rogers JW. Surf Sci 2000;453:119.
[24] Gérard JF, Le Perchec P, Pham QT. Makromol Chem 1988;189:1693.
[25] Gérard JF, Le Perchec P, Pham QT. Makromol Chem 1988;189:1719.
[26] Pourbaix M. Atlas d'équilibres électrochimiques. Gautier Villars editor, 1963.
[27] Bentadjine S. Ph.D. thesis, Université Claude Bernard, Lyon I, 1999.
[28] Bouchet J. Ph.D. thesis, Université Claude Bernard, Lyon I, 1999.
[29] Bentadjine S, Roche AA, Bouchet J. Adhesion aspects of thin films. In: Mittal KL, editor. Utrecht, NL: VSL, 2001.